

Annihilation range and final-state interaction in $\bar{p}p$ annihilation into $\pi^-\pi^+$

B. El-Bennich,^{1,*} W.M. Kloet,¹ and B. Loiseau²

¹*Department of Physics and Astronomy, Rutgers University,
136 Frelinghuysen Road, Piscataway, New Jersey 08854, USA*

²*Laboratoire de Physique Nucléaire et de Hautes Énergies (Groupe Théorie),
Université P. & M. Curie, 4 Place Jussieu, 75252 Paris Cedex 05, France*

(Dated: 29 January 2003)

The large set of accurate data on differential cross section and analyzing power from the CERN LEAR experiment on $\bar{p}p \rightarrow \pi^-\pi^+$ in the range from 360 to 1550 MeV/c is well reproduced within a distorted wave approximation approach. The initial $\bar{p}p$ scattering wave functions originate from a recent $\bar{N}N$ model. The transition operator is obtained from a combination of the 3P_0 and 3S_1 quark-antiquark annihilation mechanisms. A good fit to the data, in particular the reproduction of the double dip structure observed in the analyzing powers, requires quark wave functions for proton, antiproton, and pions with radii slightly larger than the respective measured charge radii. This corresponds to an increase in range of the annihilation mechanisms and consequently the amplitudes for total angular momentum $J = 2$ and higher are much larger than in previous approaches. The final state $\pi\pi$ wave functions, parameterized in terms of $\pi\pi$ phase shifts and inelasticities, are also a very important ingredient for the fine tuning of the fit to the observables.

PACS numbers: 12.39.Jh.; 13.75.Cs; 21.30.Fe; 25.43.+t

I. INTRODUCTION

The very accurate set of data from the LEAR experiment [1] on $\bar{p}p \rightarrow \pi^-\pi^+$ measuring the differential cross section and analyzing power from 360 to 1550 MeV/c is still a challenge for theoretical models after more than a decade. Large variations are observed in the analyzing power A_{0n} as a function of angle at all energies, indicating presence of several partial waves already at low energies. However, recent model calculations [2, 3, 4, 5, 6, 7] lead to scattering amplitudes which are strongly dominated by total angular momentum $J = 0$ and $J = 1$. The reason for this is the choice of a rather short range annihilation mechanism. The short range of the annihilation in the model calculations originates from the dynamics of baryon exchange in Refs. [2, 3, 4, 7] or from required overlap of quark and antiquark wave functions for proton and antiproton in Refs. [5, 6, 8]. On the other hand the experimental data on differential cross sections as well as those on asymmetries point to a significant $J = 2$, $J = 3$ and even higher J contributions [9, 10, 11, 12].

All above mentioned models, for this reaction, use a distorted wave approximation (DWA). The ingredients for calculating the $\bar{p}p \rightarrow \pi^-\pi^+$ amplitudes consist of **i**) the initial $\bar{p}p$ scattering wave functions $\Psi_{\bar{p}p}(\mathbf{r})$ **ii**) a transition operator $O(\mathbf{r}', \mathbf{r})$ and **iii**) the final state $\pi\pi$ wave function $\Psi_{\pi\pi}(\mathbf{r}')$. The complete scattering amplitude T itself, constructed in a DWA fashion, is

$$T = \int d\mathbf{r}' d\mathbf{r} \Phi_{\pi\pi}(\mathbf{r}') O(\mathbf{r}', \mathbf{r}) \Psi_{\bar{p}p}(\mathbf{r}). \quad (1)$$

For example in Ref. [5] the transition operator $O(\mathbf{r}', \mathbf{r})$

was obtained from a combination of 3P_0 and 3S_1 quark-antiquark annihilation model

$$O(\mathbf{r}', \mathbf{r}) = N_0 [V_{^3P_0}(\mathbf{r}', \mathbf{r}) + \lambda V_{^3S_1}(\mathbf{r}', \mathbf{r})], \quad (2)$$

where the relative strength λ is a complex parameter and N_0 an overall real normalization factor. In the same reference $\Psi_{\bar{p}p}(\mathbf{r})$ was provided by the 1982 Paris $\bar{N}N$ potential model [13] and $\Phi_{\pi\pi}(\mathbf{r}')$ was a simple plane wave. This work did not succeed in reproducing the double-dip structure of the analyzing power and the forward peak in the differential cross section as seen experimentally at, for example, 497 MeV/c. All previously mentioned models exhibit similar difficulties.

The aim of the present paper is to study possible improvements of previous models. First of all, mesonic final-state interaction should be considered. The total energy of the $\bar{p}p \rightarrow 2\pi$ reaction for the studied data set is in the 2 GeV range. In this energy region the $\pi\pi$ interaction is characterized by several resonances [14]. In Refs. [4, 6] the role of $\pi\pi$ final-state interactions was studied. In Ref. [4] some improvement was obtained using a $\pi\pi$ model reproducing the real part of the $\pi\pi$ phase shifts with inelasticity parameters in all $J \neq 0$ partial waves remaining close to 1. In Ref. [6] which explores the 3P_0 part of the quark-antiquark dynamics in the transition operator, the final-state interaction, resulting from meson exchange, affects mainly observables in the backward region. In both approaches the double-dip structure observed in experimental data of the analyzing power remains elusive and further study is still needed. Final-state interactions of two mesons in $N\bar{N}$ annihilation have also been studied, at quark level, within an extension of the quark rearrangement model [8]. Results were reported for branching ratios of decays into various two-meson channels. Unfortunately there are no predictions from this work for differential cross sections

*Electronic address: bennich@physics.rutgers.edu

or analyzing powers.

Within the approach of Ref. [5] we will study the effect of final-state interactions guided by the $\pi\pi$ coupled channel model of Ref. [15]. Secondly we will study predictions following modification of the annihilation operator $O(\mathbf{r}', \mathbf{r})$. As remarked above this operator is rather short range in all present models. The reason for the short range of $O(\mathbf{r}', \mathbf{r})$ is that in the quark-antiquark annihilation model the antiproton and proton have a relatively small radius since their quark wave functions describe only the qqq and $\bar{q}\bar{q}\bar{q}$ core ignoring the $\bar{q}q$ cloud. It could be a cause of discrepancy between theory and experiment. In Ref. [5] it has already been noticed that an increase of the annihilation range improves substantially the theoretical description of the data.

In the present work it is shown that the $\pi\pi$ final-state interaction is a very significant tool for the fine tuning of the fit to the observables. Furthermore the parameters that determine the size of protons and pions are also crucial. An increase of both proton and pion sizes, in closer agreement with their measured radii, allows for a much better fit to the experimental cross sections and analyzing powers. Expressions of the observables in term of the basic amplitudes together with the DWA ingredients are briefly recalled in Section II. The description of the final-state interaction is performed in Section III. The modifications of the range of the annihilation mechanisms are studied in Section IV. Section V presents the final results and conclusions are summarized in Section VI.

II. OBSERVABLES AND DWA INGREDIENTS

The reaction $\bar{p}p \rightarrow \pi^-\pi^+$ can be fully described in the helicity formalism by two independent helicity amplitudes $F_{++}(\theta)$ and $F_{+-}(\theta)$. The angle θ is the c.m. angle between the outgoing π^- and the incoming \bar{p} . There are four possible observables [16]

$$\frac{d\sigma}{d\Omega} = \frac{1}{2}(|F_{++}|^2 + |F_{+-}|^2), \quad (3)$$

$$A_{0n} \frac{d\sigma}{d\Omega} = \text{Im}(F_{++}F_{+-}^*), \quad (4)$$

$$A_{\ell s} \frac{d\sigma}{d\Omega} = \text{Re}(F_{++}F_{+-}^*), \quad (5)$$

$$A_{ss} \frac{d\sigma}{d\Omega} = \frac{1}{2}(|F_{++}|^2 - |F_{+-}|^2). \quad (6)$$

So far only $d\sigma/d\Omega$ and A_{0n} have been accurately measured at LEAR [1]. For completeness we recall here the partial wave expansion of the helicity amplitudes [16]

$$F_{++}(\theta) = \frac{1}{p} \sum_J \sqrt{(2J+1)/2} \times \left[\sqrt{J} f_{J-1}^J - \sqrt{J+1} f_{J+1}^J \right] \times P_J(\cos \theta), \quad (7)$$

and

$$F_{+-}(\theta) = \frac{1}{p} \sum_J \sqrt{(2J+1)/2} \times \left[\sqrt{\frac{1}{J}} f_{J-1}^J + \sqrt{\frac{1}{J+1}} f_{J+1}^J \right] \times P_J'(\cos \theta). \quad (8)$$

The indices J and $L = J \pm 1$ are the total and orbital angular momentum of the $\bar{p}p$ system respectively. $P_J(\cos \theta)$ and $P_J'(\cos \theta)$ denote a Legendre polynomial and its derivative. The angular momentum of the $\pi\pi$ system is $\ell_{\pi\pi} \equiv J$. Because of parity conservation there are no $L = J$ amplitudes in above expansion. Total isospin $I = 0$ for even J and $I = 1$ for odd J . In Eqs. (7) and (8) p is the magnitude of the antiproton center of mass (CM) momentum.

The partial wave amplitudes f_L^J for $L = J \pm 1$ are calculated following the DWA method of Eq. (1). One ingredient is the initial coupled spin-triplet $\Psi_{\bar{p}p}(\mathbf{r})$ wave function in configuration space as obtained in [17]. The operator $O(\mathbf{r}, \mathbf{r}')$ is constructed from the quark model description of protons and pions combined with the 3P_0 and 3S_1 quark-antiquark annihilation and rearrangement mechanism [5]. The last ingredient is the $\pi\pi$ scattering wave function $\Phi_{\pi\pi}(\mathbf{r}')$ which in this paper will be built according to a study of a realistic $\pi\pi$ scattering model [15], while also comparisons will be made for a simple plane wave $\pi\pi$ final state. Subsequently one obtains the differential cross section $d\sigma/d\Omega$ and the analyzing power A_{0n} or left-right asymmetry for the proton target polarized normal to the scattering plane.

III. FINAL-STATE INTERACTION

First we assume no interaction between the final pions and describe the $\pi\pi$ scattering wave function $\Phi_{\pi\pi}(\mathbf{r}')$ as a plane wave. In this case the overall normalization of $d\sigma/d\Omega$ and the relative strength λ between 3P_0 and 3S_1 annihilation mechanism are parameters to be determined through χ^2 minimization. Out of the twenty energies where polarization data are available [1] we chose a representative set of five energies, $T_{\text{lab}} = 66.7, 123.5, 219.9, 499.2$, and 803.1 MeV, corresponding to antiproton momenta of respectively $p_{\text{lab}} = 360, 497, 679, 1089$, and 1467 MeV/c. T_{lab} is the laboratory kinetic energy of the antiproton beam. At 123.5 MeV ($p_{\text{lab}} = 497$ MeV/c) and 219.9 MeV ($p_{\text{lab}} = 679$ MeV/c) we do reproduce the results of [5] using their parameters. Results for the set of five energies are shown in Figs. 1–5 as short-dashed curves. The overall fits are poor with exception of the analyzing power A_{0n} at 803.1 MeV ($p_{\text{lab}} = 1467$ MeV/c). The double-dip structure of A_{0n} is not reproduced at the three lowest energies of the set considered here, which can be attributed to the very small values of the $J \geq 2$ amplitudes predicted by this model. A lack of substantial $J \geq 2$ amplitudes is also evident in the predictions for $d\sigma/d\Omega$ at all energies. The forward peak is poorly

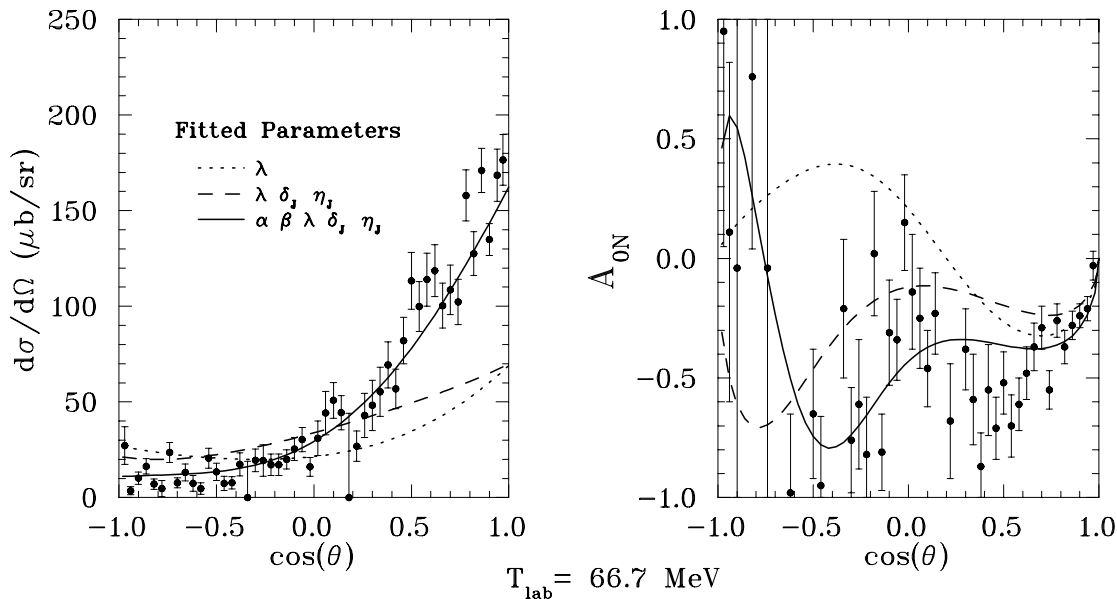


FIG. 1: Differential cross section and analyzing power of the reaction $\bar{p}p \rightarrow \pi^-\pi^+$ at $T_{\text{lab}} = 66.7$ MeV ($p_{\text{lab}} = 360$ MeV/c). Experimental data from Hasan *et al.* [1]. The different curves are described in the text.

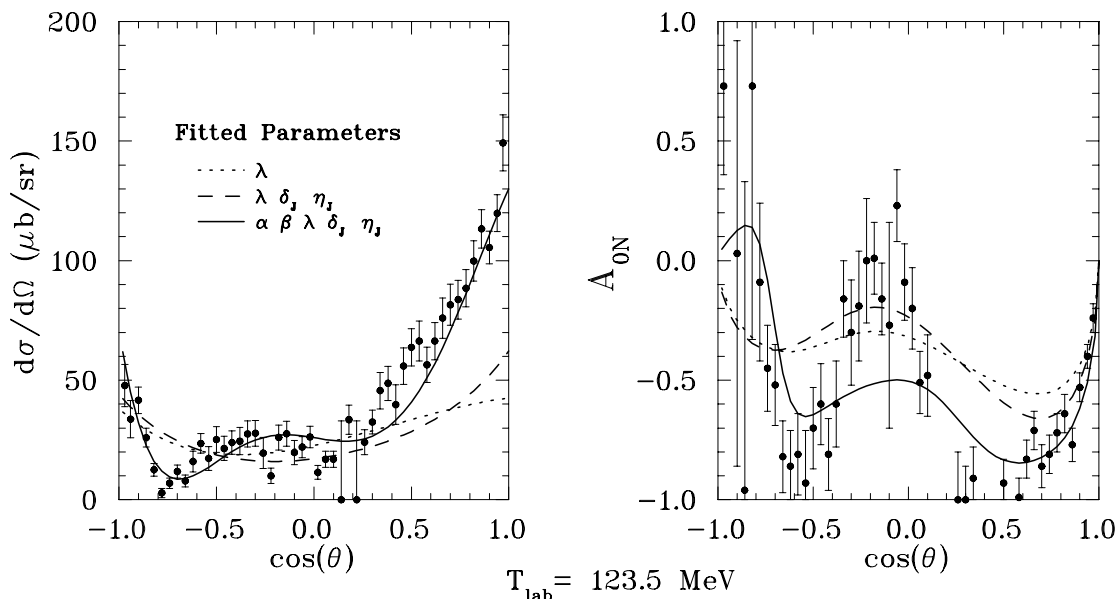


FIG. 2: As in Fig. 1 but for $T_{\text{lab}} = 123.5$ MeV ($p_{\text{lab}} = 497$ MeV/c).

reproduced, and also the backward peak, prominent in the data at $T_{\text{lab}} = 499.2$ MeV, is missing in this simplified model. Similar findings were obtained previously at $T_{\text{lab}} = 123.5$ and 219.9 MeV by [5]. As shown in the analysis of [11] we recall that large $J \geq 2$ amplitudes are needed to explain the angular dependence of A_{0n} and $d\sigma/d\Omega$.

One possibility to enhance the amplitudes of higher J values could be to introduce $\pi\pi$ final-state interaction. The elastic $\pi\pi \rightarrow \pi\pi$ amplitude is known from threshold

up to the total relativistic $\pi\pi$ energy $\sqrt{s} = 1800$ MeV mainly from analysis of the $\pi N \rightarrow \pi\pi N$ reaction. The extracted $\pi\pi \rightarrow \pi\pi$ amplitudes can be parameterized in terms of phase shifts δ_J and inelasticities η_J where $J = 0, 1, 2$ and 3 [18]. In [15] a coupled channel model of $\pi\pi$, $\bar{K}K$ and $\rho\rho$ was proposed to reproduce these phase parameters δ_J and η_J for $J = 0, 1, 2$ and 3. The $\Phi_{\pi\pi}(\mathbf{r}')$ wave functions required for the final-state interaction of $\bar{p}p \rightarrow \pi\pi$, can be constructed from this coupled channel model in a straightforward manner. However, since the

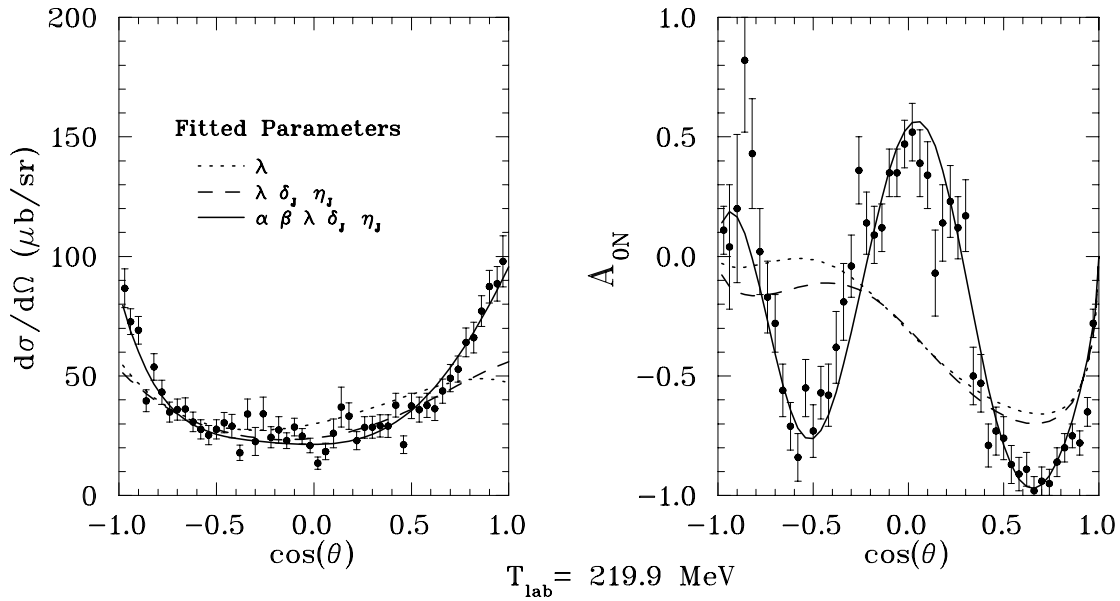


FIG. 3: As in Fig. 1 but for $T_{\text{lab}} = 219.9 \text{ MeV}$ ($p_{\text{lab}} = 679 \text{ MeV}/c$).

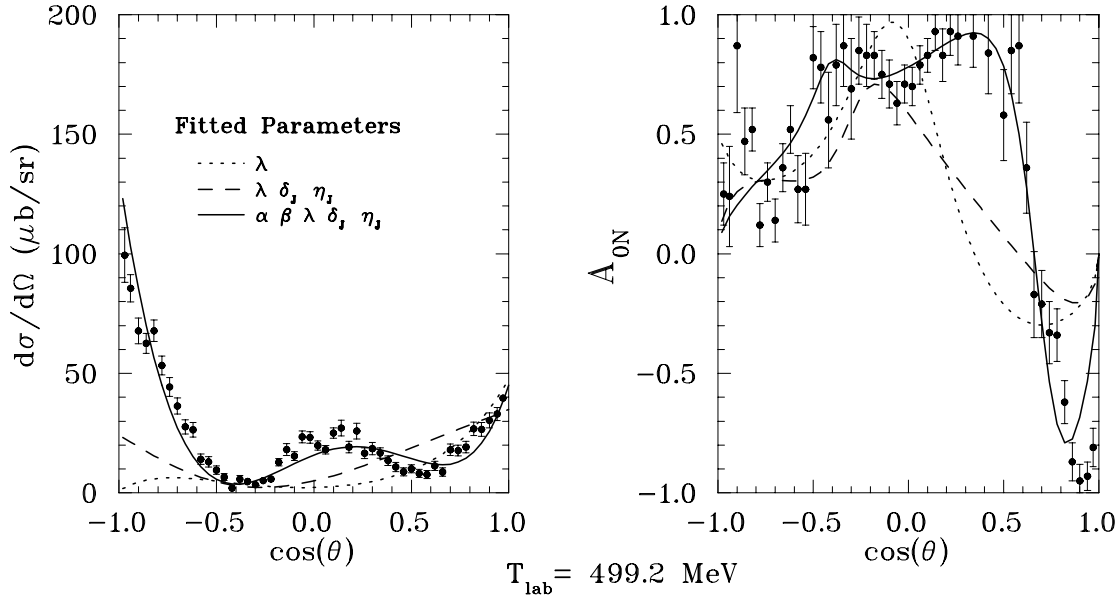


FIG. 4: As in Fig. 1 but for $T_{\text{lab}} = 499.2 \text{ MeV}$ ($p_{\text{lab}} = 1089 \text{ MeV}/c$).

needed energy range in $\bar{p}p \rightarrow \pi\pi$ is from $\sqrt{s} = 1910$ to 2272 MeV one has to rely on extrapolation of the coupled channel model results beyond $\sqrt{s} = 1800 \text{ MeV}$. Calculations with the corresponding $\Phi_{\pi\pi}(\mathbf{r}')$ show a significant sensitivity of the observables to the $\pi\pi$ final-state interaction. Even so the $\pi\pi$ scattering amplitude from the extrapolated coupled channel $\pi\pi$ model still does not improve the predictions of $\bar{p}p \rightarrow \pi\pi$ obtained previously with $\pi\pi$ plane waves. But in this study we did find that the off-shell part of $\Phi_{\pi\pi}(\mathbf{r}')$ does play a very minor role. In particular it was observed that the same predictions of

observables $d\sigma/d\Omega$ and A_{0n} can be obtained using only the asymptotic part of the $\pi\pi$ wave functions. We then exploit this fact by asserting for the remainder of this paper that in $\bar{p}p \rightarrow \pi\pi$ the unknown $\pi\pi$ final-state scattering can be fully described by the asymptotic $\pi\pi$ wave functions parameterized by the $\pi\pi$ phases δ_J and inelasticities η_J .

We then avoid the problem of extrapolation to high \sqrt{s} by including these new parameters δ_J and η_J in the minimization process to obtain realistic fits to $d\sigma/d\Omega$ and A_{0n} . Results of this second fitting procedure are shown

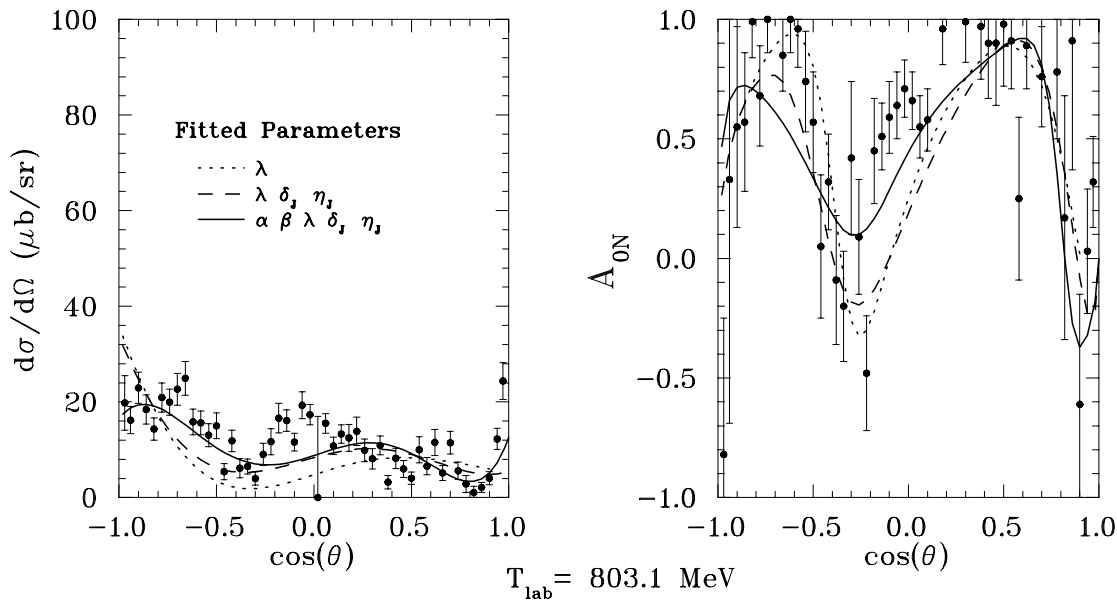


FIG. 5: As in Fig. 1 but for $T_{\text{lab}} = 803.1$ MeV ($p_{\text{lab}} = 1467$ MeV/c).

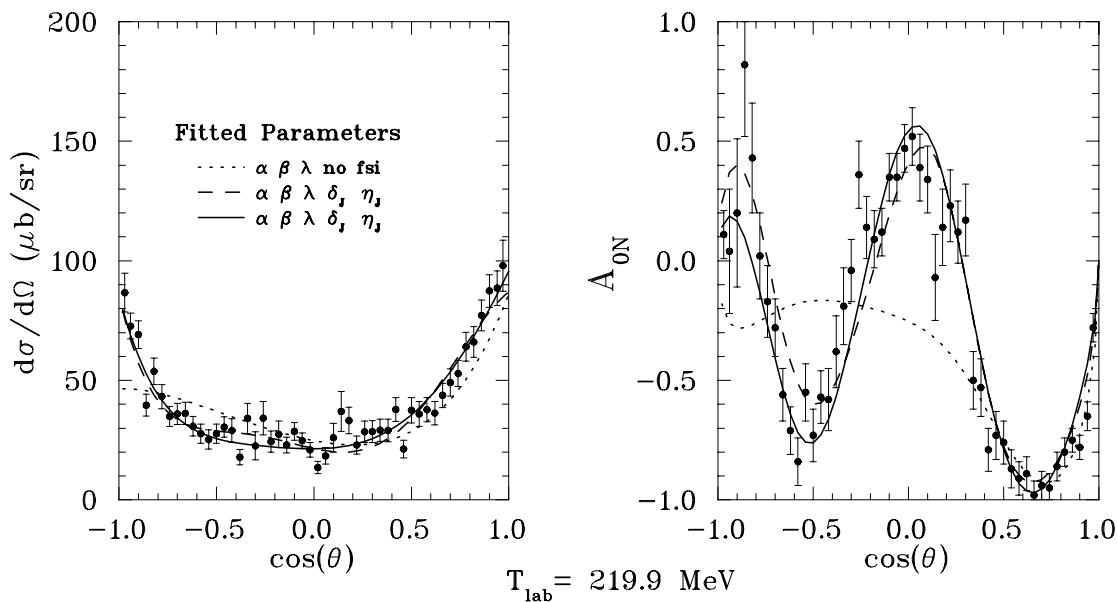


FIG. 6: Various fits for $T_{\text{lab}} = 219.9$ MeV ($p_{\text{lab}} = 679$ MeV/c). The solid curve is as in Fig. 3. The long-dashed curve represents a fit with final-state interaction, where $\alpha = 1.09 \text{ fm}^{-2}$ and $\beta = 1.51 \text{ fm}^{-2}$. The short-dashed curve is a fit with no final-state interaction, where $\alpha = 1.27 \text{ fm}^{-2}$ and $\beta = 1.53 \text{ fm}^{-2}$.

as the long-dashed curves in Figs. 1–5. Switching on final state $\pi\pi$ interaction improves the fit of A_{0n} by readjusting the strength of the helicity amplitudes of different J . This allows for prediction of a double-dip structure at lower energies. This feature is a crucial requirement of the data and shows the need for incorporating the final-state interaction of the pions in some form. However the predictions for $d\sigma/d\Omega$ show only a modest improvement over the model without final-state interaction and

the question arises whether there is additional freedom within the model to ameliorate the present fit. So far, the only variable parameter in the annihilation operator is the relative strength λ unless one allows variations of the range of the annihilation mechanism controlled by the parameters α and β [5]. In the next section we will investigate the effects of variations in α and β .

IV. MODIFICATION OF THE ANNIHILATION RANGE

In order to derive the annihilation operator $O(\mathbf{r}', \mathbf{r})$ (2), one can describe the proton, antiproton and pions in terms of quarks and antiquarks with the use of Gaussian wave functions [5]. This amounts to approximate quark confinement by solving the Dirac equation with either a scalar or vector harmonic oscillator potential. The proton (antiproton) intrinsic wave function for the annihilation mechanism is :

$$\psi_N(\mathbf{r}_1, \mathbf{r}_2, \mathbf{r}_3) = N_N \exp \left[-\frac{\alpha}{2} \sum_{i=1}^3 (\mathbf{r}_i - \mathbf{r}_N)^2 \right] \times \chi_N(\text{spin, isospin, color}), \quad (9)$$

where \mathbf{r}_i are the quark (antiquark) coordinates and \mathbf{r}_N the nucleon (antinucleon) coordinate. An S -wave meson intrinsic wave function is:

$$\phi_M(\mathbf{r}_1, \mathbf{r}_4) = N_M \exp \left[-\frac{\beta}{2} \sum_{i=1,4} (\mathbf{r}_i - \mathbf{r}_M)^2 \right] \times \chi_M(\text{spin, isospin, color}). \quad (10)$$

Here \mathbf{r}_1 and \mathbf{r}_4 are the quark and antiquark coordinates, respectively. The coordinate of the meson is \mathbf{r}_M .

Typical parameter values used before are $\alpha = 2.80 \text{ fm}^{-2}$ and $\beta = 3.23 \text{ fm}^{-2}$ which correspond to a proton (antiproton) radius of 0.60 fm and a meson radius of 0.48 fm [19]. This value of α describes the qqq ($\bar{q}\bar{q}\bar{q}$) core of the proton (antiproton) while the measured charge radius, which for the proton is about 0.8 fm, includes also the mesonic cloud. Explicit expressions in terms of α and β for the transition operators $V_{3P_0}(\mathbf{r}', \mathbf{r})$ and $V_{3S_1}(\mathbf{r}', \mathbf{r})$ of Eq. (2) can be found in [5]. However, one can also argue that in modeling the Gaussian wave functions as in Eqs. (9) and (10), values for α and β simply should be in accordance with known charge radii of the proton and pion. The measured pion charge distribution radius [20] is $\langle r_\pi^2 \rangle^{1/2} = 0.663 \pm 0.006 \text{ fm}$. For the proton we find $\langle r_p^2 \rangle^{1/2} = 0.870 \pm 0.008 \text{ fm}$ in the literature [14]. We are thus left with a certain freedom when it comes to choosing values for α and β and we can wonder about the effects on the annihilation mechanism. The values of the parameters α and β determine effectively the range of the annihilation mechanism. Let us assume we increase the size of the proton and the pion from their original values in [5] by decreasing α and β . Then the integration over the intrinsic quark coordinates of, for example, the wave functions $\psi_p(\mathbf{r}_1, \mathbf{r}_2, \mathbf{r}_3)$, $\psi_{\bar{p}}(\mathbf{r}_4, \mathbf{r}_5, \mathbf{r}_6)$, $\phi_{\pi^+}(\mathbf{r}_1, \mathbf{r}_4)$, and $\phi_{\pi^-}(\mathbf{r}_2, \mathbf{r}_5)$ will result in a larger quark overlap. The corresponding annihilation operator $O(\mathbf{r}', \mathbf{r})$ will have a longer range and therefore higher partial waves will contribute to the total amplitude \mathbf{T} in Eq. (1) as required by the analyses of experimental data of Refs. [9, 10, 11, 12].

Changes of α and β can furthermore be linked to relativistic corrections of the pion wave function $\phi_M(\mathbf{r}_1, \mathbf{r}_4)$

as the outgoing energy of the pion is much larger than its rest mass. In practical terms this means that in the center of mass, where the calculation is performed, the pion wave function should not be described as a sphere anymore. A proper treatment requires a Lorentz boost of the pion intrinsic wave function from its rest frame to the CM frame. Thus one expects a change in the geometry of the Gaussian shape of the pion [21]. This affects the overlap integral (1) which could be mocked by a simultaneous alteration of α and β . We therefore take α and β to be variable parameters to the extent that they still satisfy physical conditions.

V. FINAL FIT

The results of our final fit which includes now values of the parameters α , β , $\lambda = |\lambda| \exp(i\theta_\lambda)$, δ_J , η_J , and of the overall normalization N_0 are shown as solid curves in Figs. 1–5. The improvement over the previous fits is dramatic but requires both increased sizes of the antiproton, proton and pions as well as a tuned final-state interaction. The main achievement is the reproduction in the differential cross section $d\sigma/d\Omega$ of the characteristic forward peaks at lower energies ($T_{\text{lab}} = 66.7, 123.5$ and 219.9 MeV) and backward peaks at higher energies ($T_{\text{lab}} = 219.9$ and 499.2 MeV). This clearly indicates that the increase of the annihilation range now produces much larger amplitudes for $J = 2$ and higher. The predictions for the double-dip structure of the analyzing power A_{0n} compare much better with the experimental results especially for $T_{\text{lab}} \geq 219.9 \text{ MeV}$.

In addition to the double-dip structure of A_{0n} the experimental data display another characteristic feature: the asymmetry shifts from predominantly negative values at lower energies toward positive values at higher energies. Our final fit accounts for this pattern. The quark model parameters α , β , λ , and the overall norm N_0 resulting from this fit are listed in Table I and the phase shifts δ_J and inelasticities η_J of the final-state interaction with their dependence on \sqrt{s} in Table II. Note that the latter have been readjusted in the final fit and differ from the δ_J and η_J obtained in the fit presented in section III. The $\pi\pi$ phases for $J = 0, 1$ are small but for $J = 2, 3, 4$ they are substantial. The inelasticities η_J , in particular for $J = 2$ may indicate the presence of resonances in this channel. From Table I it is also clear that the parameters α and β are almost constant with energy but have lower values at 219.9 MeV. Nevertheless, in Fig. 6 we show (long-dashed line) that one can obtain a fit of similar quality keeping the size parameters $\alpha = 1.09 \text{ fm}^{-2}$ and $\beta = 1.51 \text{ fm}^{-2}$ close to the ones at the other four energies. The relative strength λ exhibits an energy dependence. This dependence shows a smooth decrease of $|\lambda|$ with increasing \sqrt{s} , which indicates that the 3P_0 mechanism preponderates at higher energies. The phase θ_λ of λ should be compared with the value $\theta_\lambda = 180^\circ$ of [5]. Furthermore, we find that

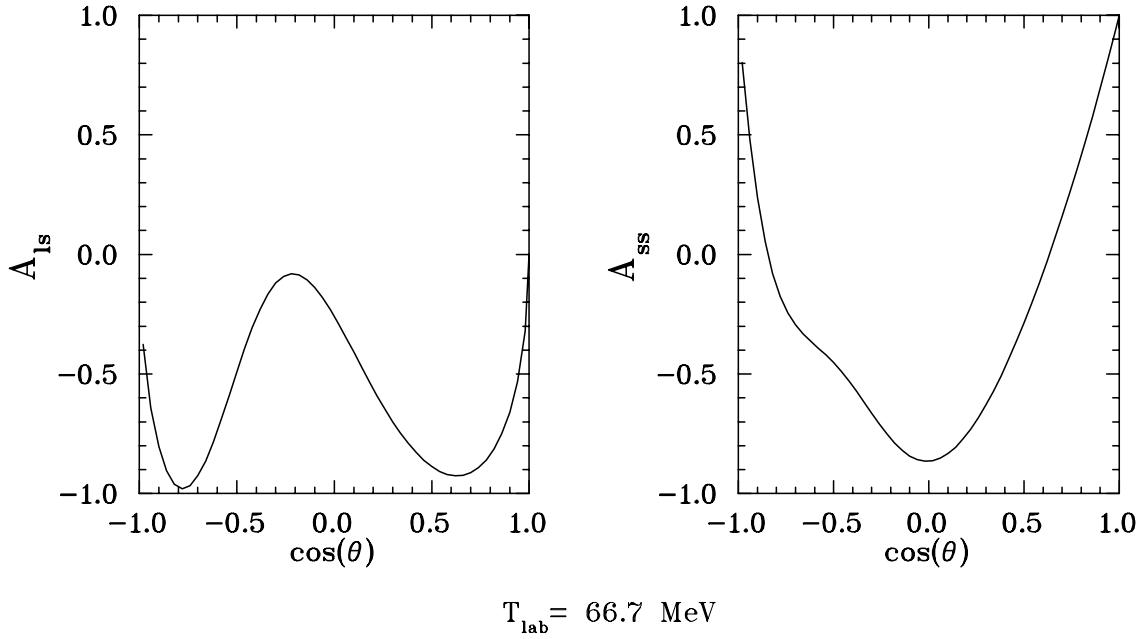


FIG. 7: Predictions at $T_{\text{lab}} = 66.7 \text{ MeV}$ ($p_{\text{lab}} = 360 \text{ MeV}/c$) for the observables $A_{\ell s}$ and A_{ss} obtained with the final fit.

α decreases by about a factor 2.3 while β decreases by about 2.2. In other words, the proton size in this model increases to $\langle r_p^2 \rangle^{1/2} = 0.91 \text{ fm}$ and the pion radius is now $\langle r_\pi^2 \rangle^{1/2} = 0.71 \text{ fm}$, which is within 7% of the values of references [14] and [20] mentioned in the previous section.

The dramatic improvement that occurs when the size parameters α and β take on smaller values, tends to mask the equally important role of the final-state interaction. If the final-state interaction is turned off from the very beginning by fixing the phase parameters $\delta_J = 0$ and $\eta_J = 1$ while α, β, λ are allowed to vary, α and β again decrease significantly, which confirms an increased annihilation range within our model. Nevertheless, the resulting fit without final-state interaction is far from satisfactory and it is only when we include final-state interaction that we recover the fit quality discussed earlier in this section. This is illustrated at $T_{\text{lab}} = 219.9 \text{ MeV}$ ($p_{\text{lab}} = 679 \text{ MeV}/c$) in Fig. 6. The short-dashed curve represents the fit without final-state interaction, and for which $\alpha = 1.27 \text{ fm}^{-2}$ and $\beta = 1.53 \text{ fm}^{-2}$. This short-dashed curve in

$T_{\text{lab}} [\text{MeV}]$	66.7	123.5	219.9	499.2	803.1
$p_{\text{lab}} [\text{MeV}/c]$	369	497	679	1089	1467
$\alpha [\text{fm}^{-2}]$	1.20	1.19	1.11	1.20	1.20
$\beta [\text{fm}^{-2}]$	1.54	1.51	1.00	1.54	1.54
$ \lambda $	1.200	1.064	0.662	0.545	0.424
$\theta_\lambda [^\circ]$	197.10	125.68	166.83	176.32	183.29
$N_0 [10^5]$	5.251	4.804	5.046	4.222	4.667

TABLE I: Quark model parameters as function of T_{lab} .

Fig. 6 should be compared with the short-dashed curve in Fig. 3 for which $\alpha = 2.80 \text{ fm}^{-2}$ and $\beta = 3.23 \text{ fm}^{-2}$. The differential cross section has improved significantly in the forward hemisphere. However the analyzing power is only marginally better. The solid line of Fig. 6 is with inclusion of the final-state interaction. Similar results are obtained at the other energies, which confirms that in order to reproduce the LEAR data both an increased annihilation range as well as interaction in the final $\pi\pi$ state is necessary.

With the present parameters, we can proceed to compute other spin observables for the $\bar{p}p \rightarrow \pi^-\pi^+$ reaction. We take the opportunity to present for each energy considered above the predictions for the spin observables $A_{\ell s}$

$T_{\text{lab}} [\text{MeV}]$	66.7	123.5	219.9	499.2	803.1
$\sqrt{s} [\text{MeV}]$	1910.	1937.	1983.	2111.	2242.
η_0	0.840	0.989	0.937	1.00	1.00
δ_0	-4.57	-4.37	-6.59	-5.24	-0.63
η_1	0.998	0.995	0.921	0.999	0.914
δ_1	8.05	4.89	-4.14	-3.24	-1.88
η_2	0.756	0.669	0.760	0.818	0.309
δ_2	35.74	24.49	55.57	37.66	74.95
η_3	1.00	1.00	0.808	1.00	1.00
δ_3	59.66	41.41	62.45	48.15	-19.59
η_4	1.00	0.997	0.858	1.00	0.990
δ_4	36.93	-41.29	6.19	-60.70	61.77

TABLE II: Phases shifts δ_J and inelasticities η_J of the final-state interaction for $0 \leq J \leq 4$ as function of \sqrt{s} .

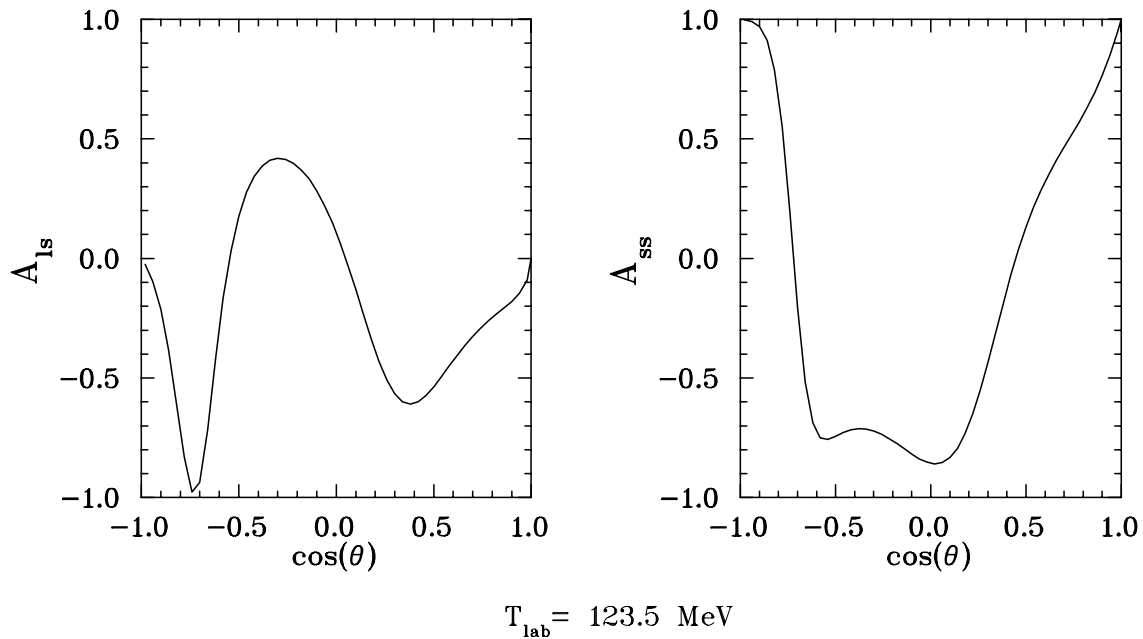


FIG. 8: As in Fig. 7 but for $T_{\text{lab}} = 123.5 \text{ MeV}$ ($p_{\text{lab}} = 497 \text{ MeV}/c$).

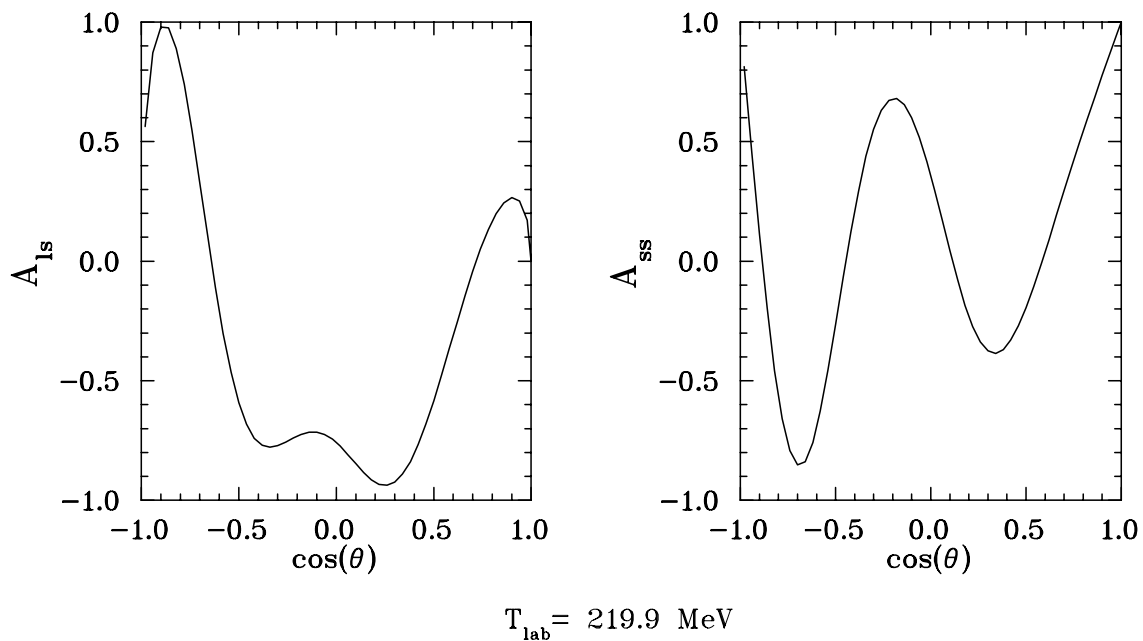


FIG. 9: As in Fig. 7 but for $T_{\text{lab}} = 219.9 \text{ MeV}$ ($p_{\text{lab}} = 679 \text{ MeV}/c$).

and A_{ss} introduced in Eqs. (5) and (6). We remind the reader that the spin observables are related by

$$A_{0n}^2 + A_{\ell s}^2 + A_{ss}^2 = 1, \quad (11)$$

and that the reaction $\bar{p}p \rightarrow \pi^- \pi^+$ has only three independent observables within a sign ambiguity, and of course $d\sigma/d\Omega$ is chosen as one of them. At each energy the corresponding parameters of Tables I and II are used. The

results are shown in Figs. 7–11. The spin observables $A_{\ell s}$ and A_{ss} exhibit again the typical structure with two extrema as a function of angle, which take often the form of a double dip. There is as yet no data to compare with.

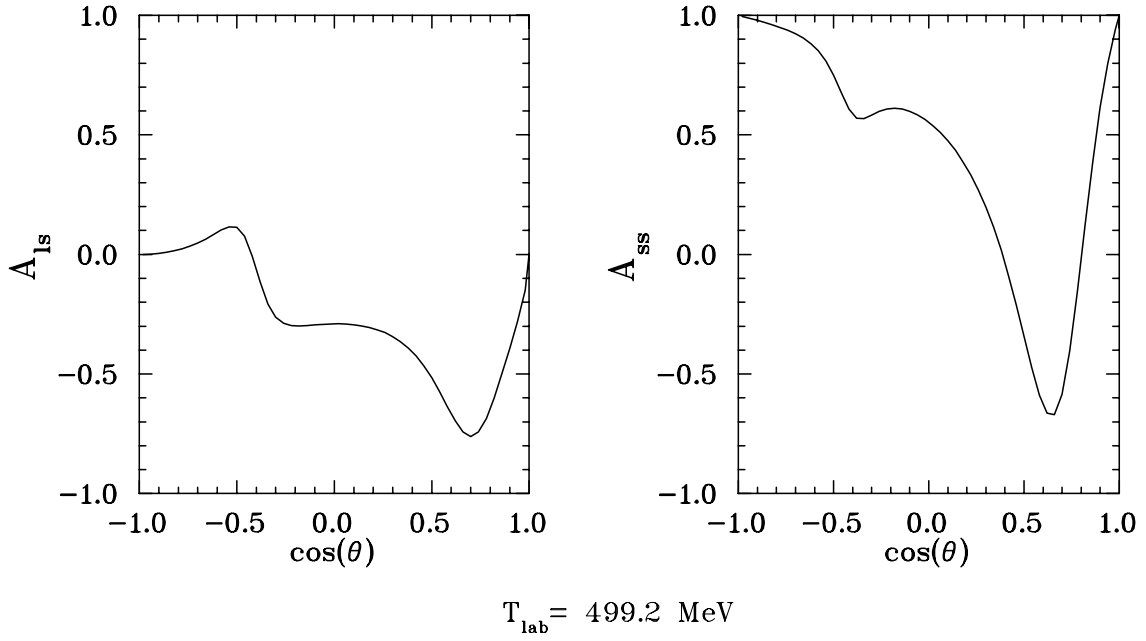


FIG. 10: As in Fig. 7 but for $T_{\text{lab}} = 499.2 \text{ MeV}$ ($p_{\text{lab}} = 1089 \text{ MeV/c}$).

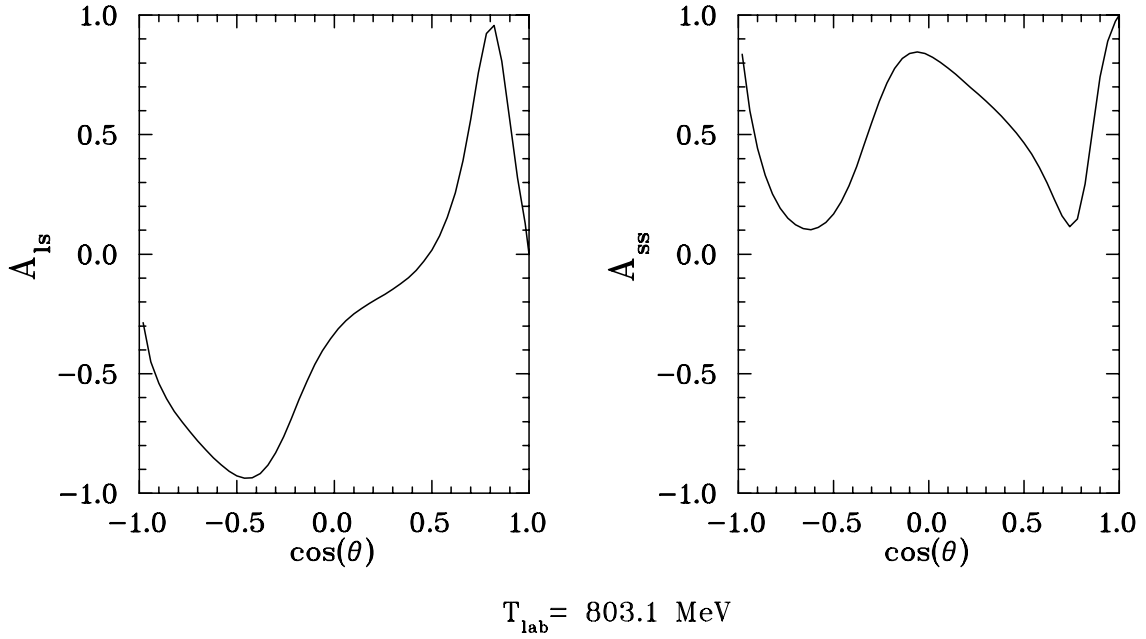


FIG. 11: As in Fig. 7 but for $T_{\text{lab}} = 803.1 \text{ MeV}$ ($p_{\text{lab}} = 1467 \text{ MeV/c}$).

VI. CONCLUSION

The extensive set of data of differential cross sections $d\sigma/d\Omega$ and analyzing powers A_{0n} from the LEAR experiment [1] on $\bar{p}p \rightarrow \pi^-\pi^+$ in the range $p_{\text{lab}} = 360$ to 1550 MeV/c can be fitted by the combined mechanisms 3P_0 and 3S_1 of the quark-antiquark annihilation model.

The initial $\bar{p}p$ relative wave functions were taken from [17]. It is important to include the final state $\pi\pi$ interaction and employ quark wave functions for proton, antiproton, and pions with radii which are slightly larger than the respective measured charge radii. Previously used hadron intrinsic quark wave functions [5] describe only the quark core of the hadrons without the $\bar{q}q$ cloud and their parameters therefore correspond to a consid-

erably smaller radius. Increased hadronic radii lead to an increase in range of the annihilation mechanism and as a result amplitudes for $J = 2$ and higher are much larger than before. This feature in the model is essential since the experimental data on A_{0n} exhibit a double dip, which indicates the presence of substantial amplitudes of $J = 2$ and higher, already at lower momenta p_{lab} . The relative strength of the 3P_0 and 3S_1 mechanisms shows a smooth energy dependence and suggests that the 3P_0 mechanism becomes more dominant at the higher energies. It is however noted that the pronounced forward and backward peaks in the cross section require the presence of both 3P_0 and 3S_1 mechanisms.

Acknowledgments

B.E. and W.M.K. thank the LPNHE and its Groupe Théorie for their warm and stimulating hospitality. B.L. wishes to acknowledge the welcome and support of the Department of Physics and Astronomy of Rutgers University during his visits. Laboratoire de Physique Nucléaire et de Hautes Énergies is Unité de Recherche des Universités Paris 6 et Paris 7 associée au CNRS. This research was supported in part by the U.S. National Science Foundation Phy-9722088.

-
- [1] *Differential cross sections and analyzing powers for $\bar{p}p \rightarrow \pi^-\pi^+$ and K^-K^+ from 360 to 1550 MeV/c*, A. Hasan, D.V. Bugg, J.R. Hall, R.L. Shypit, F. Tesarotto, R. Birsas, F. Bradamante, S. Dalla Torre-Colautti, A. Martin, A. Menzo *et al.*, Nucl. Phys. **B378**, 3 (1992).
 - [2] *$\bar{N}N$ annihilations into two mesons*, B. Moussallam, Nucl. Phys. **A407**, 413 (1983); *$\bar{p}p \rightarrow \pi^-\pi^+$ in a baryon exchange potential model*, B. Moussallam, Nucl. Phys. **A429**, 429 (1984).
 - [3] *Meson-baryon dynamics in the nucleon-antinucleon system II. Annihilation into two mesons*, V. Mull, J. Haidenbauer, T. Hippchen, and K. Holinde, Phys. Rev. C **44**, 1337 (1991).
 - [4] *The role of final-state interactions in the $\bar{p}p \rightarrow \pi^-\pi^+$ annihilation process*, V. Mull, K. Holinde, and J. Speth, Phys. Lett. B **275**, 12 (1992).
 - [5] *Left-right asymmetry in $\bar{p}p \rightarrow \pi^-\pi^+$* , G. Bathas and W.M. Kloet, Phys. Rev. C **47**, 2207 (1993); *Generalized 3P_0 and 3S_1 annihilation potentials for $\bar{p}p$ decay into two mesons based on a simple quark model*, G. Bathas and W.M. Kloet, Phys. Lett. B **301**, 155 (1993).
 - [6] *$p\bar{p}$ -annihilation into two mesons in the quark annihilation model including final state interaction*, A. Muhm, T. Gutsche, R. Thierauf, Y. Yan, and Amand Faessler, Nucl. Phys. **A598**, 285 (1996).
 - [7] *Role of tensor meson pole and Δ exchange diagrams in $\bar{p}p \rightarrow \pi^-\pi^+$* , Y. Yan and R. Tegen, Phys. Rev. C **54**, 1441 (1996); *Baryon exchange and meson pole diagrams in $\bar{p}p \rightarrow \bar{K}K, \pi^-\pi^+$* , Y. Yan and R. Tegen, Nucl. Phys. **A648**, 89 (1999).
 - [8] *NN annihilation into two mesons, effect of final-state interactions*, A.M. Green and G.Q. Liu, Nucl. Phys. **A486**, 581 (1988).
 - [9] *Amplitude analysis of data on $\bar{p}p \rightarrow \pi^-\pi^+$ at low energy*, M.N. Oakden and M.R. Pennington, Nucl. Phys. **A574**, 731 (1994).
 - [10] *Amplitudes for $\bar{p}p \rightarrow \pi^-\pi^+$ from 0.36 GeV/c to 2.5 GeV/c*, A. Hasan and D.V. Bugg, Phys. Lett. B **334**, 215 (1994).
 - [11] *Amplitude analysis of the $\bar{N}N \rightarrow \pi^-\pi^+$ reaction*, W.M. Kloet and F. Myhrer, Phys. Rev. D **53**, 6120 (1996).
 - [12] *Partial-wave amplitudes and resonances in $\bar{p}p \rightarrow \pi + \pi$* , B.R. Martin and G.C. Oades, Phys. Rev. C **56**, 1114 (1997); *Amplitudes and resonances from an energy-dependent analysis of $\bar{p} + p \rightarrow \pi + \pi$* , B.R. Martin and G.C. Oades, Phys. Rev. C **57**, 3492 (1998).
 - [13] *Nucleon-Antinucleon Optical Potential*, J. Côté, M. Lacombe, B. Loiseau, B. Moussallam, and R. Vinh Mau, Phys. Rev. Lett. **48**, 1319 (1982).
 - [14] *Review of particle physics*, K. Hagiwara *et al.* (Particle Data Group), Phys. Rev. D **66** (2002) 010001.
 - [15] *$\pi\pi$ scattering and the meson resonance spectrum*, W.M. Kloet and B. Loiseau, Eur. Phys. J. A **1**, 337 (1998).
 - [16] *Determination of, and resonance structure in, the $\bar{p}p$ to $\pi\pi$ partial waves*, A.D. Martin and M.R. Pennington, Phys. Lett. B **86**, 93 (1979); *Exploration of the $\bar{p}p \rightarrow \pi\pi$ channel in the resonance region*, A. D. Martin and M. R. Pennington, Nucl. Phys. **B169**, 216 (1980).
 - [17] *Refining the inner core of the Paris NN potential*, B. El-Bennich, M. Lacombe, B. Loiseau, and R. Vinh Mau, Phys. Rev. C **59**, 2313 (1999).
 - [18] *$\pi\pi$ Partial-Wave Analysis from Reactions $\pi^+p \rightarrow \pi^+\pi^-\Delta^{++}$ and $\pi^+p \rightarrow K^+K^-\Delta^{++}$ at 7.1 GeV/c*, S. Protopopescu *et al.*, Phys. Rev. D **7**, 1279 (1973); *High statistics study of the reaction $\pi^-p \rightarrow \pi^+\pi^-n$: apparatus, method of analysis and general features of results at 17 GeV/c*, G. Grayer *et al.*, Nucl. Phys. **B75**, 189 (1974); *A study of the $\pi\pi$ phase-shift solutions in the mass region 1.0 to 1.8 GeV from $\pi^-p \rightarrow \pi^-\pi^+n$ at 17.2 GeV*, B. Hyams *et al.*, Nucl. Phys. **B100**, 205 (1975); *Experimental study of 30000 K_{e4} decays*, L. Rossetlet *et al.*, Phys. Rev. D **15**, 574 (1977); *New results on $\pi\pi$ phase shifts between 600 and 1900 MeV*, D. V. Bugg, A. V. Sarantsev, and B. S. Zou, Nucl. Phys. **B471**, 59 (1996); *Separation of S-wave pseudoscalar and pseudovector amplitudes in $\pi^-p \uparrow \rightarrow \pi^+\pi^-n$ reaction on polarized target*, R. Kamiński, L. Leśniak, and K. Rybicki, Acta Phys. Pol. C **74**, 79 (1997); *Further study of the $\pi\pi$ S-wave isoscalar amplitude below the $K\bar{K}$ threshold*, R. Kamiński, L. Leśniak, and K. Rybicki, Acta Phys. Pol. B **31**, 895 (2000); *A new measurement of K_{e4}^+ decay and the S-wave $\pi\pi$ -scattering length a_0^0* , S. Pislak *et al.* (E865 Coll.), Phys. Rev. Lett. **87** (2001) 221801; *A joint analysis of the S-wave in the $\pi^+\pi^-$ and $\pi^0\pi^0$ data*, R. Kamiński, L. Leśniak, and K. Rybicki, Eur. Phys. J. direct C **4**, 1 (2002).
 - [19] *$p\bar{p}$ annihilation in an s wave quark rearrangement model*,

- A.M. Green and J.A. Niskanen, Nucl. Phys. **A412**, 448 (1984); *$p\bar{p}$ annihilation in a quark rearrangement model including s and p waves*, *ibid.* **A430**, 605 (1984); *The p wave triplet versus s wave triplet for quark-antiquark annihilation*, Mod. Phys. Lett A **1**, 441 (1986).
- [20] *A measurement of the space-like pion electromagnetic form-factor*, S. Amendolia *et al.*, Nucl. Phys. **B277**, 168 (1986).
- [21] *Relativistic corrections in $\bar{p}p \rightarrow \pi^-\pi^+$* , B. El-Bennich and W. M. Kloet, in preparation (2003).